| ![ESRF logo] | **Experiment title:** Accelerating connectomics by combining X-ray nanotomography with electron microscopy | **Experiment number**: LS-2705 |
|---|---|---|
| **Beamline**: ID16A-NI | **Date of experiment**: from: Sept 13, 2017 to: Sept 17, 2017 | **Date of report**: Mar 27, 2018 |
| **Shifts: 12** | **Local contact(s)**: JOITA PACUREANU Alexandra<br>Tel: +33 4 38 88 19 52<br>Email: joitapac@esrf.fr | *Received at ESRF:* |

**Names and affiliations of applicants** (* indicates experimentalists):

Kuan, Aaron[1], Maniates-Selvin, Jasper[1], Somhegyi, Hannah[1], Lee, Wei-Chung[1,2]
[1]Department of Neurobiology, Harvard Medical School, Boston, MA, USA
[2]F.M. Kirby Neurobiology Center, Boston Children's Hospital, Boston, MA, USA

## Report:

In this experiment, we used X-ray phase-contrast nanoscale tomography to study the structure of the nervous system of the adult fruit fly *Drosophila melanogaster*. We tested a wide array of sample preparation protocols, identified preparations that produced the high quality datasets, and succesfully scanned and reconstructed several regions of the fly nervous system. To our knowledge, these datasets are the highest resolution X-ray reconstructions of neural circuits to date, allowing us to trace the morphologies of large and medium sized neuronal processes. We also demonstrated that it is possible to combine electron microscopy (EM) and X-ray reconstruction on the same samples. **Our results from this experiment have demonstrated that sub-100 nm resolution X-ray phase contrast nanotomography of neural circuits provides a rapid method of large-volume, moderate-resolution circuit reconstruction that can readily be complemented with high-resolution serial section electron microscopy to enable the detailed study of structure and connectivity in neuronal circuits.** Datasets obtained in this experiment are already being analyzed to help understand neural circuits involved in hearing and walking (**Fig. 3,4**). Additionally, we are currently preparing a manuscript describing the methods developed in this experiment to help inform the neuroscience community about the power of studying neuronal circuits with nanoscale X-ray phase-contrast tomography. Here, we report in more detail on three topics: (1) Optimal sample preparation conditions, (2) Successful scans and assessments of data quality, and (3) Challenges in achieving <50nm resolution and high contrast, along with possible steps to achieve this in future experiments.

### 1. Sample preparation

We aimed to produce samples that are compatible with both X-ray phase contrast imaging and EM. We prepared tissue samples from the adult fly with several different protocols, and compared imaging quality and contrast. The following parameters were tested:

**Tissue type:** (1) brain (2) nerve cord (3) antenna (4) leg (**Fig. A**). We found that individual neurons could be reconstructed in all 4 tissue types, despite the different tissue types having dramatically different anatomical structures.

**Staining:** (1) unstained (2) minimally heavy-metal stained (3) maximally heavy-metal stained. We found that ample X-ray phase contrast could be acquired from all samples, even those with no staining. We have also performed EM on stained samples and demonstrated that both light and heavy staining protocols are suitable for both EM and X-ray imaging.

**Embedding:** (1) epoxy resin block trimmed with a diamond knife (**Fig. 1a**) (2) epoxy resin droplet (**Fig. B, 3a**) (3) paraffin wax trimmed with a razor blade (**Fig 2a**). We found that diamond-trimmed samples contain micron-scale surface roughness, which introduced image artifacts. To avoid this issue, we developed a new technique of embedding samples in droplets of epoxy resin to produce samples with very smooth surfaces (Fig. B). This enabled acquisition of X-ray images without artifacts. Droplet embedding and will be the embedding of choice for future experiments.

## 2. Successful scans and assessment of data quality:

We performed tomographic scans at room temperature with 17keV X-ray energy, with voxel sizes ranging from 30 to 130 nm. Images were recorded at 2048x2048 pixels, resulting in fields-of-view ranging from 61 to 266 μm. In most scans, we captured projections of the sample from 2000 angles at each of 4 different sample-to-detector distances, totaling 8000 projections acquired over a ~4 hour period. Some scans were then successfully reconstructed into phase contrast volumes using tomographic reconstruction. Here we describe a few example datasets.

**1) Central brain:** We prepared a sample of the fly's brain that was maximally heavy-metal stained, which is ideal for EM (**Fig. 1a**). We performed and reconstructed scans at 120 (**Fig.1b**) and 70 nm voxels (**Fig. 1c**). In order to demonstrate that EM can be performed on the same samples after X-ray imaging, we performed EM on thin sections from brains prepared with the same protocol (**Fig. 1d**). In these X-ray reconstructions, large axons in the brain can be followed for long distances, but many neurons remain too small to reliably traced.
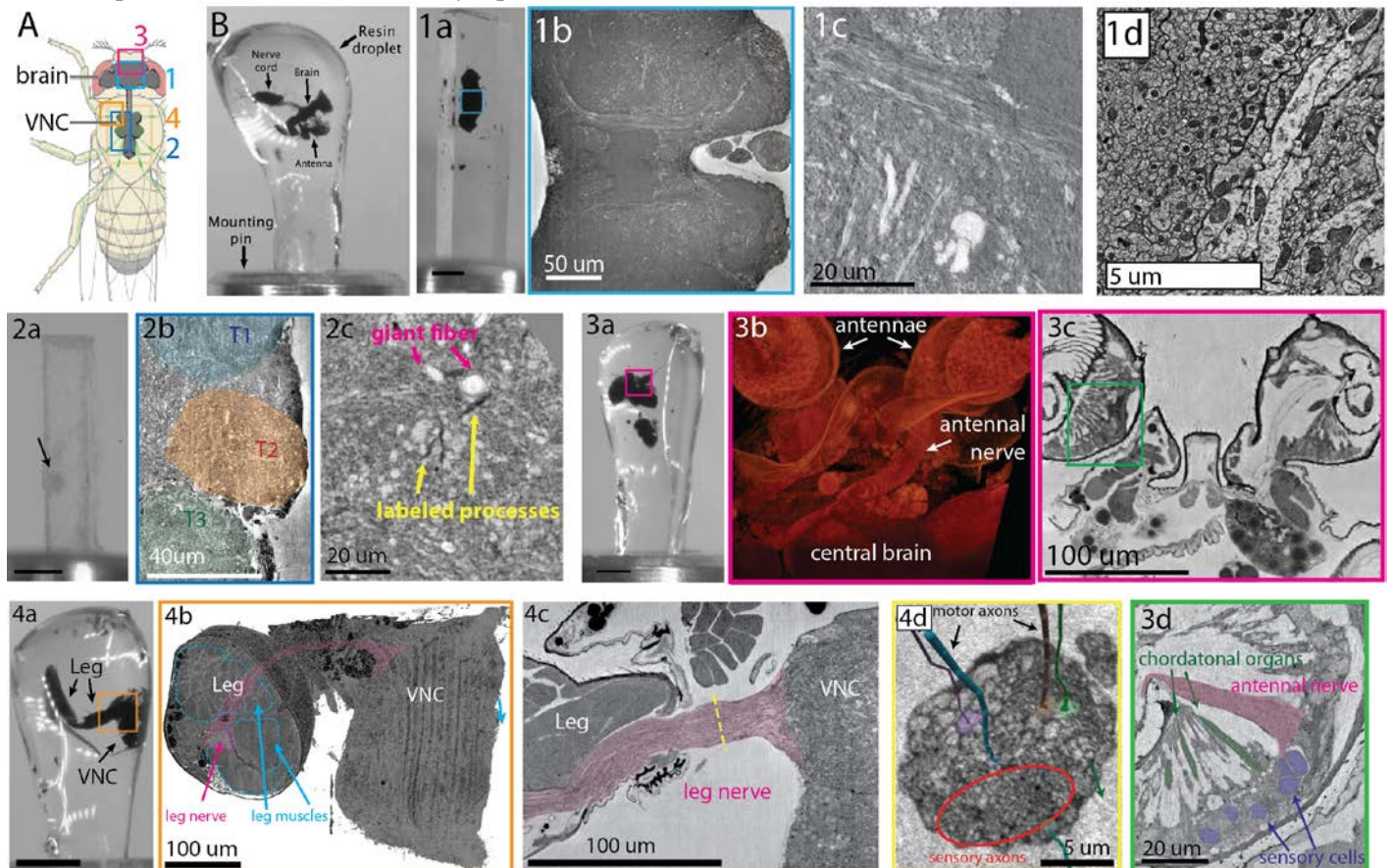
**2) Ventral nerve cord (VNC):** We prepared an unstained nerve cord sample embedded in paraffin wax (**Fig. 2a**). Using genetic tools, we targeted a dense precipitate to certain neurons known to be involved in turning decisions. These neurons should appear dark in X-ray and EM images (**Fig. 2c**, yellow arrows). We performed 4 scans at different voxel sizes: 110, 80, 40, and 25 nm. We successfully reconstructed the 110 (**Fig. 2b**) and 80 nm (**Fig. 2c**) scans, but reconstructions of higher resolution scans appeared blurred. In the reconstructed volumes, cell bodies can be seen clearly and and large axons (**Fig. 2c**, magenta arrows) can be followed for long distances. Most neurons in the nerve cord are too small to trace with the resolution we achieved, but this is to our knowledge the first demonstration of neuron tracing in X-ray reconstructions of an unstained sample. Furthermore, we likely identified the genetically labeled neurons (**Fig 2c**, yellow arrows), but this has not yet been confirmed by an independent methods (e.g. confocal or electron microscopy).

**3) Antenna and anterior central brain:** We prepared a minimally heavy-metal stained sample of the fly's two antennae attached to the central brain (**Fig. 3a**). The antenna contains sensory organs that detect sound and wind, but these organs are surrounded in exoskeleton, making them difficult to physically section for studying with EM. Therefore, X-ray imaging is an ideal modality for studying the fly antennae and other peripheral organs. We performed several scans in an effort to reconstruct the sensory neurons in the antenna, the axons of those neurons traveling to the brain, and the regions in the central brain where the axons split into branches. We succeeded in acquiring and reconstructing several partially-overlapping volumes that can be stitched together: a 130 nm voxel scan containing both antennae and part of the brain (**Fig. 3b,c**), a 60 nm voxel scan of one antenna and its sensory neurons (**Fig. 3d**), a 60 nm voxel scan of the axons traveling to the brain, and a 90 nm voxel scan of the part of the brain containing these axons. We also acquired a scan of the brain at 40 nm, but this dataset could not be reconstructed due to sample warping during imaging. The 60 nm dataset of the antenna had sufficient resolution to see the morphology of individual sensory neurons and chordatonal organs (**Fig. 3d**, arrows)**.** This was the highest resolution dataset we successfully reconstructed, likely due to the large amount of empty space inside and around the antenna, which reduced the amount of X-ray absorption and warping. The axons of the antenna's sensory neurons could be followed short distances toward the brain, but the resolution needs further improvement in order to trace individual axons all the way into the brain. Because of this, we are focusing our analysis on the antenna itself, in order to determine how the position of each sensory neuron enables it to respond to different frequencies of sound.

**4) Leg and Lateral Ventral Nerve Cord (VNC):** We prepared a minimally heavy-metal stained sample containing one leg attached to the ventral nerve cord (**Fig. 4a**). We imaged portions of the nerve cord and the attached leg at 190 nm (**Fig. 4b**), 100 nm (**Fig. 4c**), 80 nm, and 60 nm (**Fig. 4d**) voxels. In these reconstructions, it is straightforward to trace individual motor neurons from the leg to the VNC (**Fig. 4d**, colored rods). However, in addition to motor axons, there are also smaller sensory axons that send sensory signals from the leg to the VNC. In our reconstructions, these sensory axons were not resolvable. Despite imaging with voxels as small as 60 nm, the effective resolution was not better than 100 nm to due to reconstruction artifacts caused by sample heating and deformation during imaging. In proposed follow-up experiments, we hope utilized cryogenic imaging to image an entire leg at sufficient resolution to trace both motor and sensory axons.

## 3. Challenges in achieving higher resolution:

Contrast could be improved for most brain and nerve cord samples acquired with small (<100 nm) voxels. These often contained severe reconstruction artifacts persumably caused by warping due to heating form the high X-ray flux. Two of our samples developed bubbles and cracks that expanded during scans, making reconstructions impossible. Decreasing exposure time can mitigate warping, at the cost of decreased signal-to-noise. We observed that acquisitions in the brain and nerve cord with pixel sizes less than 90 nm displayed warping and low contrast, but the antenna and leg samples, which have lower overall density, displayed good contrast down to 60 nm pixel sizes. In discussions with the beamline scientists at ID16A, we have identified two approaches to achieve better resolution and contrast in future experiments: (**1**) **Unbinned imaging**: The detector used by ID16A is actually 4096-by-4096 pixels, but typically data is acquired at 2x binning to increase signal-to-noise and reduce scan times. During our experiment, we acquired some preliminary unbinned datasets (4096 pxels), which may allow us to resolve more fine features in our samples. Currently, beamline ID16A's beamline scientists are modifying the tomographic reconstruction software to allow reconstruction of these unbinned data acquisitions. (**2**) **Cyrogenic imaging**: The ID16A beamline has the capability to perform imaging in cryogenic conditions, which significantly decreases sample heating, and presumably warping. Furthermore, the sample stage is also more stable at cryogenic temperatures. Given that reconstruction artifacts were a significant challenge in our first experiment, we see cryogenic imaging as a promising next step to improve the stability of our samples and the quality of our datasets. Because we can already resolve large neurons in our room temperature X-ray imaging datasets, any improvements brought about by cryogenic imaging should dramatically increase the number of neurons we can resolve. We anticipate this will enable nanoscale X-ray imaging to become an important tool for research into the structure of neurons and neuronal circuits, potentially resolving not only fine neuronal processes, but also even the synaptic connections between them.



**Experimental Figures.** (**A**) Diagram of central nervous system of adult fly. Regions of interest are outlined: 1) central brain 2) ventral nerve cord (VNC) 3) antennae 4) leg. (**B**) Stained fly central nervous system prepared in a resin droplet for X-ray phase-contrast nanotomography.
(**1**) **Central Brain.** 1a) Photograph of sample mounted for tomographic imaging. Scale bar: 500 um. 1b) Example slice from 120 nm voxel volume reconstruction. 1c) Close-up of slice from 70 nm voxel volume reconstruction. 1d) Thin-section electron microscopy image of sample prepared identically as shown in 1a, demonstrating the feasibility of EM and X-ray imaging with the same sample preparation. (**2**) **Unstained VNC.** 2a) Photograph of sample mounted for tomographic image. Scale bar: 500 um. 2b) Example slice of 100 nm voxel volume reconstruction. 2c) Close-up slice from 80 nm voxel volume reconstruction. Large axons and putative genetically-labeled processes are resolved. (**3**) **Antennae and Anterior Central Brain.** 3a) Photograph of sample mounted for tomographic reconstruction. Scale bar: 500 um. 3b) 3-D rendering of 130 nm voxel reconstruction containing 2 antennae, antennal nerve, and part of the central brain. 3c) Example slice of 130 nm voxel volume reconstruction. 3d) Close-up slice of 60 nm voxel volume reconstruction of a single antennal segment. Sensory cells and their corresponding chordatonal organs are resolvable. (**4**) **Leg and Lateral VNC.** 4a) Photograph of sample mounted for tomographic reconstruction. Scale bar: 500 um. 4b) 3-D rendering of 190 nm voxel overview scan containing portions of the leg and connected VNC. 4c) Example slice from 100 nm voxel volume reconstruction, showing nerve connecting leg to VNC. 4d) Close-up slice of 60 nm voxel reconstruction of leg nerve. Motor neuron axons are clearly resolvable (colored pipes). Smaller, sensory neuron axons are not resolvable (red oval).